Two-Way Synchronization for Coordinated Multicell Retrodirective Downlink Beamforming

Robert D. Preuss, *Senior Member, IEEE*, and D. Richard Brown, III, *Senior Member, IEEE*

***Abstract*—Coordinated multicell downlink transmission has recently been proposed as a technique that can enable spectrally efficient communication in cellular networks. By coordinating downlink transmissions, the base stations in a cellular system can transmit such that signals from multiple base stations arrive coherently at a mobile. One approach to coordinated multicell downlink transmission is to have the mobiles estimate the downlink channel state information (CSI) and feed the CSI back to the base stations for precoding. This paper proposes a different approach based on retrodirectivity and channel reciprocity. The primary advantage of this approach is that there is no need for CSI estimation or feedback by the mobiles. A tradeoff, however, is that the base stations must be synchronized to within a small fraction of a carrier period. A new two-way base station synchronization protocol is proposed to facilitate coordinated multicell coherent retrodirective downlink transmission techniques. An analysis of the statistical properties of the estimation errors in the two-way synchronization protocol and the resulting power gain of a multicell retrodirective downlink beamformer using this protocol is provided. Numerical examples are also presented characterizing the performance of multicell retrodirective downlink beamforming in a system using two-way base station synchronization. The numerical results demonstrate that near-ideal multicell downlink beamforming performance can be achieved with low synchronization overhead.**

***Index Terms*—Antenna arrays, base station coordination, carrier frequency synchronization, carrier phase synchronization, cellular radio, distributed beamforming, multicell wireless networks, synchronization.**

I. Introduction

CELLULAR communication systems are based on the principle that a large geographic area can be divided into several smaller geographic areas called "cells," each comprising a base station wirelessly communicating with the mobile terminals in the cell. At any point in time, each mobile typically communicates with a single base station in the system. As a mobile moves through the system, the wireless communication link is handed off from base station to base station so that, roughly speaking, the mobile is always communicating with the nearest base station.

In some cellular systems, a technique called "soft handoff" [1] is used in situations where a mobile is near the boundary between cells. Soft handoff increases the reliability of communication in cellular systems by allowing a mobile to maintain communication with two or more base stations when it does not have a strong channel to a single base station. The gain in reliability is a consequence of *diversity* since the mobile receives two copies of the same message through different channels. Soft handoff is an example of a simple *multicell* communication technique that increases communication reliability and decreases mobile power consumption.

Recently, more sophisticated multicell communication techniques have been proposed in which multiple base stations effectively operate as a distributed antenna array. By increasing the level of coordination among the base stations, well-known multi-input multi-output (MIMO) transmission techniques can be used in the system to increase sum capacity, decrease downlink interference, and/or direct downlink transmissions toward individual mobiles in the network, e.g., distributed beamforming. An early study of coordinated multicell downlink transmission appeared in [2] where it was shown that a fourfold capacity increase could be achieved through phase and amplitude control across the base stations in the cellular network. Distributed downlink beamforming and greedy scheduling was studied in coordinated cellular networks in [3] and [4]. The spectral efficiency and maximum common rate of coordinated downlink transmission was analyzed in [5]–[10].

One compelling motivation for the development of *coherent* coordinated multicell downlink transmission techniques is that the received power at the mobile can grow proportional to the *square* of the number of transmitting antennas when the passband signals arrive in phase. This is in contrast with incoherent multicell downlink transmission, e.g., soft handoff, where the power at the mobile grows only linearly in the number of transmitting antennas. Incoherent multiantenna transmission can provide a *diversity gain*, but it does not provide a *beamforming gain*.

In the coordinated multicell downlink transmission system described in [11], coherent downlink transmission was achieved by synchronizing the base stations, having the mobiles in the network estimate the downlink channel state information (CSI), and having the mobiles feed their CSI back to the base stations for phase alignment via precoding. The time and frequency synchronization requirements for this approach were discussed in

Manuscript received January 26, 2011; revised May 18, 2011; accepted June 28, 2011. Date of publication July 18, 2011; date of current version October 12, 2011. The associate editor coordinating the review of this manuscript and approving it for publication was Dr. Biao Chen. This work was supported by the NSF award CCF-0447743. The material in this paper was presented at the 44th Annual Conference on Information Sciences and Systems (CISS 2010), March 17-19, 2010.

R. D. Preuss is with Raytheon BBN Technologies, Cambridge, MA 02138 USA (e-mail: rpreuss@bbn.com).

D. R. Brown, III, is with the Electrical and Computer Engineering Department, Worcester Polytechnic Institute, Worcester, MA 01609 USA (e-mail: drb@ece.wpi.edu).

Color versions of one or more of the figures in this paper are available online at http://ieeexplore.ieee.org.

Digital Object Identifier 10.1109/TSP.2011.2162329

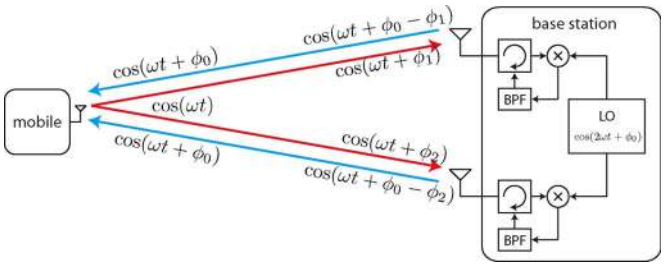

Fig. 1. An example of the principle of operation of a conventional retrodirective two-antenna Pon array.

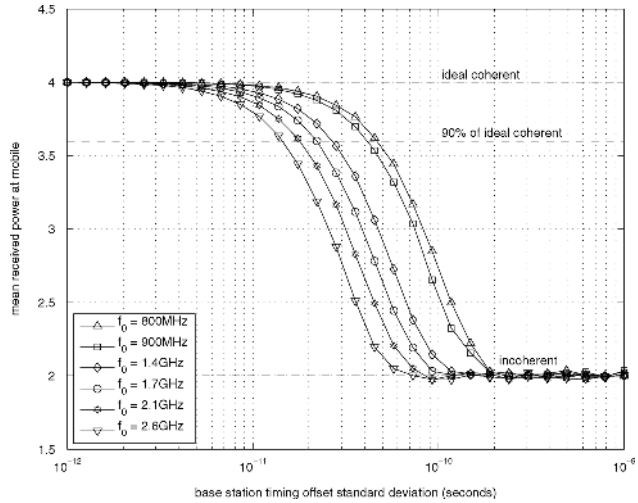

Fig. 2. The effect of base station timing offset on the mean received power at the mobile for the case when $M = 2$ base stations attempt to transmit as a retrodirective distributed beamformer to the mobile.

[12] where the time synchronization requirements were shown to be relatively loose (a fraction of the symbol period) and the frequency synchronization requirements were shown to be relatively stringent (on the order of one part per billion) in the scenarios considered.

A drawback of the approach described in [11] is that the mobiles must continuously estimate the downlink channel state and feed the CSI back to the base stations. The processing required for CSI estimation may lead to increased cost and reduced battery life for the mobiles. The feedback overhead can also be significant, e.g., on the order of megabits per second [11], even in small networks.

In this paper, we consider a different approach to coherent coordinated multicell downlink transmission that does not require CSI estimation or feedback by the mobiles. The approach is based on retrodirectivity and channel reciprocity. Fig. 1 illustrates the principle of operation of a two-antenna conventional retrodirective antenna array (the Pon array [13]). In Fig. 1, the uplink signal from the mobile is received by each antenna element at potentially different phases. These received signals are mixed with the base station's local oscillator, running at twice the frequency of the uplink carrier. The bandpass filter at each antenna rejects the high frequency 3ω term and passes the ω term, effectively conjugating the channel and forming a coherent beam back to the mobile as a consequence of uplink/downlink channel reciprocity.

In our proposed distributed implementation of coordinated multicell retrodirective downlink beamforming, each base station mixes the received uplink signal with its own local oscillator. The base stations' local oscillators must be closely synchronized in both phase and frequency for retrodirective transmission to achieve coherence of the passband signals at the mobile. Local oscillator offsets of more than a small fraction of a carrier period will lead to incoherent combining of the passband signals at the mobile. Fig. 2 shows the received power at the mobile for a retrodirective beamforming system as a function of base station timing offset and carrier frequency. Even at the lowest common cellular carrier frequency of 800 MHz, the standard deviation of the base stations' timing offsets must be smaller than 50 picoseconds in order to achieve, on average, 90% or better of the ideal coherent received power at the mobile. At typical GPS timing accuracies, i.e., 1 ns or more, the carriers combine incoherently and retrodirective distributed beamforming is not possible.

The main contribution of this paper is the development of a new synchronization technique called *two-way* synchronization [14] to facilitate multicell retrodirective downlink beamforming. Unlike GPS, two-way synchronization is an endogenous synchronization technique that can satisfy the subcarrier-period timing accuracies required for retrodirective distributed beamforming. Two-way synchronization can also be used to refine GPS timing estimates and/or maintain synchronization during periods of GPS outage. The two-way synchronization protocol is similar to the time-slotted round-trip distributed beamforming technique [15] in that beacons are exchanged serially, but there are several important differences including:

1) Round-trip distributed beamforming works on the principle that beacons can be exchanged over certain "round-trips" through the network, always beginning and ending at the destination, such that the propagation time (or phase shift) accumulated over each round-trip is identical. After the round-trip beacons are exchanged, the source nodes in a round-trip distributed beamformer are not actually synchronized in the sense that they would agree on the time of occurrence of an event. Instead, each source's carrier is offset with respect to the other sources' carriers such that all of the carriers combine coherently at the intended destination *after propagation*. In other words, the sources in a round-trip distributed beamformer are not synchronized, but their carriers arrive in phase alignment after propagation to the destination. Two-way carrier synchronization operates on different principle. Like master-slave open-loop [16] carrier synchronization, the goal of two-way carrier synchronization is to precisely synchronize the carriers of the sources in the system (modulo the carrier period). Distributed beamforming can then be achieved through well-known retrodirective transmission techniques, e.g., the Pon array [13].
2) Round-trip distributed beamforming begins with the transmission of a primary beacon from the intended destination. Secondary beacons are then serially exchanged among the sources to generate appropriate carrier frequencies and phases at each source, after which distributed

beamforming can commence. Two-way synchronization, on the other hand, is performed among the sources *prior* to the transmission of a beacon from the intended destination. Distributed beamforming can occur immediately after the reception of the beacon from the destination, hence a two-way synchronized distributed beamformer can provide lower latency than round-trip distributed beamforming.

3) Since round-trip distributed beamforming does not actually synchronize the source nodes, round-trip distributed beamforming in a system with multiple destination nodes requires the full set of synchronization beacons (primary and secondary) to be exchanged among the sources *for each destination node in a system*. In systems using two-way synchronization, the presynchronization beacons exchanged among the sources are the same regardless of the number of destination nodes. Only the uplink beacon must be transmitted for each destination node in the system. Hence, the overhead associated with two-way synchronization can be less than round-trip synchronization in systems with multiple destination nodes. This feature is particularly appealing in the downlink cellular scenario.

This paper provides an explicit description of the two-way carrier synchronization technique in a system where each base station keeps its own local time and uses only local estimates. We also show how channel conjugation can be performed using well-known retrodirective transmission techniques to enable multicell retrodirective downlink beamforming at an intended mobile in the cellular system. We then analyze the statistical properties of the two-way synchronization protocol in terms of the estimation errors and oscillator phase noise. We conclude with numerical examples that show that the two-way synchronization can facilitate near-ideal downlink distributed beamforming and that the associated overhead can be small with respect to the expected useful beamforming time.

II. System Model

We consider the cellular system shown in Fig. 3 with M base stations and N mobiles. Each base station and each mobile is assumed to possess a single[1] isotropic antenna. Uplink and downlink transmissions are assumed to be separated by time-division-duplexing (TDD). The multipath channel from mobile n to base station m is modeled as a linear time-invariant (LTI) system with impulse response $g_{n,m}(t)$. The noise in each channel is additive, white, and Gaussian.

We assume the base stations are connected by a backhaul to a mobile switching center (MSC) and that this backhaul is of sufficient capacity and of low enough delay such that all of the base stations within the uplink reception neighborhood of a particular mobile have a copy of the baseband messages to be transmitted in the downlink to this mobile. We also assume that a TDD "synchronization channel" between base station m and base station m' exists and this synchronization channel is a linear time-invariant (LTI) system with impulse response $h_{m,m'}(t)$. The noise in each synchronization channel is additive, white, and Gaussian.

[1]Our focus on single antennas is motivated by clarity of exposition. The synchronization and distributed beamforming techniques developed in this paper can be extended to the case where each base station has more than one antenna at the expense of some additional notational complexity.

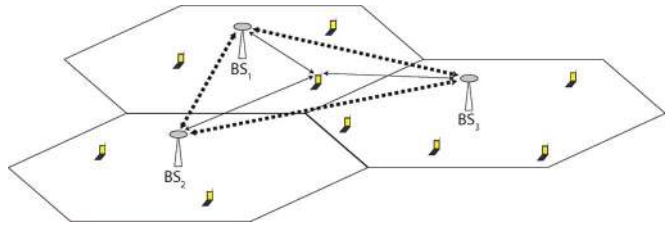

Fig. 3. A cellular system with M base stations and N mobiles, each with a single antenna. The thick dashed lines represent the "synchronization channels" between pairs of base stations and the solid lines represent the TDD uplink/downlink channel between each base station and the mobile. Not shown is the backhaul between the base stations that serves the function of distributing a common baseband message for downlink transmission.

The synchronization channel between each pair of base stations could, in principle, be achieved over the backhaul if the backhaul channel between each pair of base stations is LTI and if the backhaul itself supports the transmission of analog sinusoidal synchronization beacons as described in Section III. Cellular backhauls, however, are typically realized over digital DS-1 or E-1 links [17], [18]. These digital links are not LTI due to timing jitter in the transport and higher layers of the protocol. Moreover, these digital links do not allow for the transmission of analog beacons. In this case, and as is assumed in the rest of this paper, the synchronization channels are established through LTI wireless links between pairs of base stations.

Since all of the channels in the system are TDD, we assume channel reciprocity in each link. Basic electromagnetic principles have long established that channel reciprocity holds at the antennas when the channel is accessed at the same frequency in both directions [19]. Channel reciprocity can also be quite accurate at intermediate-frequency (IF) and/or baseband if a reciprocal transceiver architecture is used [20] and can be further improved through transceiver calibration techniques to remove I/Q imbalance effects [21], [22].

A key assumption in this paper is that the base stations do not possess a common time reference, at least not one with the accuracy needed for coherent coordinated multicell retrodirective downlink transmission. The following section presents a model of local and reference time that will be subsequently used in the description and analysis of the two-way synchronization protocol.

A. Reference Time and Local Time

A focus of this paper is the description and analysis of a carrier synchronization technique for base stations in a cellular network. To support this focus, it is necessary to explicitly present a model of local time at each base station and describe how the local time at each base station relates to a notion of "reference" time. Throughout this paper, we will use the notation t to refer to the reference time, i.e., the "true" time, in the system. All time-based quantities such as propagation delays and/or frequencies are specified in reference time unless otherwise noted.

We assume none of the base stations know the reference time t. Even if the base stations have access to a GPS time reference,

as discussed previously, the inaccuracy of GPS time is usually more than a carrier period at typical cellular frequencies. The local time at BS_i is modeled as

$$t_i = \beta_i(t + \Delta_i(t)) \tag{1}$$

where β_i represents the nominal relative rate of the clock at BS_i with respect to the reference time and $\Delta_i(t)$ is a zero-mean lowpass random process that captures the effect of fixed local time offset, local oscillator phase noise, and frequency instability [23] in the oscillator at BS_i.

Since each base station keeps its own local time and none of the base stations know the reference time, it should be emphasized that all processing in any synchronization technique must be performed using local time.

III. Two-Way Base Station Synchronization Protocol

The two-way base station synchronization protocol requires the M base stations in the cellular system to be ordered as $\{\mathsf{BS}_1, \ldots, \mathsf{BS}_M\}$. Synchronization is initiated by BS_1 transmitting a sinusoidal beacon to BS_2. Although this wirelessly transmitted beacon is of a broadcast nature and may be overheard by other base stations in the system, it is ignored by all base stations except BS_2. This sinusoidal beacon is retransmitted through increasing base station indices $\mathsf{BS}_2 \rightarrow \mathsf{BS}_3 \rightarrow \cdots \rightarrow \mathsf{BS}_{M-1} \rightarrow \mathsf{BS}_M$ ("forward propagation"), where each retransmission is a *periodic extension* of the beacon received in the previous timeslot and only the subsequent base station in the ordering receives the transmission. A second sinusoidal beacon, initiated by BS_M, is similarly transmitted through the decreasing base station indices $\mathsf{BS}_M \rightarrow \mathsf{BS}_{M-1} \rightarrow \cdots \rightarrow \mathsf{BS}_2 \rightarrow \mathsf{BS}_1$ ("backward propagation"). Assuming approximately the same frequency is used for the forward and backward propagated beacons, $2M-2$ nonoverlapping time slots (enumerated as $\mathsf{TS}^{(1)}, \ldots, \mathsf{TS}^{(2M-2)}$) are used to ensure there is no mutual interference among the $2M-2$ individual transmissions in the two-way base station synchronization protocol.

An overview of the two-way base station synchronization protocol is shown in Fig. 4. To facilitate analysis of this protocol, we assume the beacons are transmitted over a short enough interval such that the frequency and phase noise of the local oscillators is constant, i.e., $\Delta_i(t) \equiv \Delta_i$. The local time at BS_i during two-way synchronization can then be written as

$$t_i = \beta_i(t + \Delta_i). \tag{2}$$

The signals exchanged and estimates generated in each timeslot are explicitly described for the forward propagation stage as follows. In $\mathsf{TS}^{(1)}$, BS_1 transmits a sinusoidal beacon $x_1^{(1)}(t_1) = \exp\{j(\omega_1 t_1 + \phi_1)\}\mathbb{I}_{t_1 \in T_1^{(1)}}$ to BS_2 where $T_1^{(1)}$ is the transmission interval of BS_1 in $\mathsf{TS}^{(1)}$, ω_1 is the radian frequency of the transmission, and ϕ_1 is the phase of the transmission when $t_1 = 0$. Note that $x^{(1)}(t_1)$ is expressed in local time for BS_1. This beacon propagates through the LTI channel to BS_2 and is received in local time at BS_2 as

$$y_2^{(1)}(t_2)$$

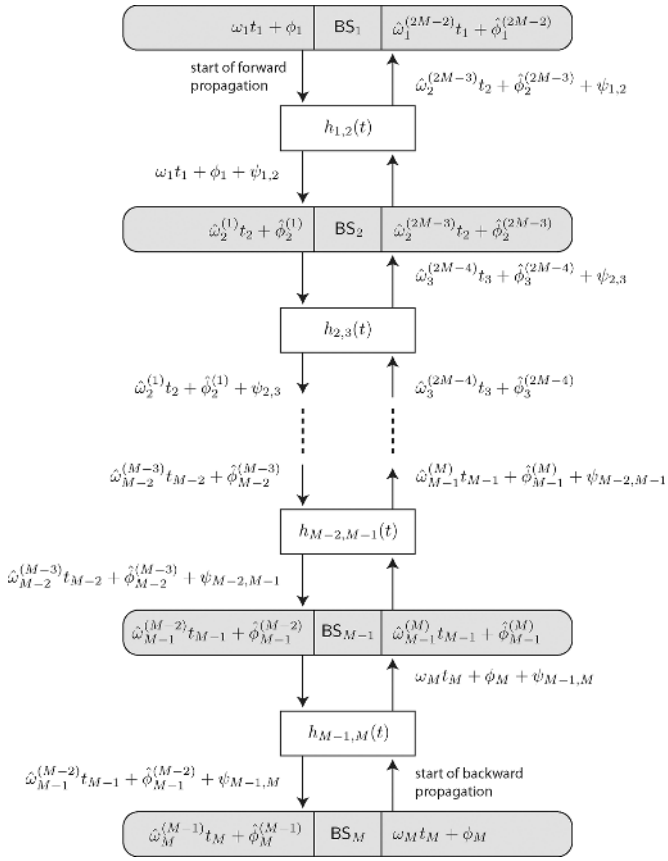

Fig. 4. Overview of the two-way base station synchronization protocol. Forward and backward propagation stages are represented with the downward and upward arrows, respectively.

$$= a_{1,2} \exp\left\{ j\left(\beta_1\omega_1 \left(\frac{t_2}{\beta_2} + \Delta_1 - \Delta_2 \right) + \psi_{1,2} + \phi_1 \right) \right\} \mathbb{I}_{t_2 \in T_2^{(1)}} + w_2^{(1)}(t_2)$$

where $T_2^{(1)}$ is the reception interval of BS_2 in $\mathsf{TS}^{(1)}$, $a_{1,2} = |H_{1,2}(\beta_1\omega_1)|$ and $\psi_{1,2} = \angle H_{1,2}(\beta_1\omega_1)$ are the amplitude and phase shift, respectively, of the LTI channel between BS_1 and BS_2 at the true frequency $\beta_1\omega_1$, and $w_2^{(1)}(t_2)$ is the noise in the signal received by BS_2 in $\mathsf{TS}^{(1)}$. This observation is then used by BS_2 to generate frequency and phase estimates

$$\hat{\omega}_2^{(1)} = \frac{\beta_1\omega_1 + \tilde{\omega}_2^{(1)}}{\beta_2}, \quad \text{and} \tag{3}$$

$$\hat{\phi}_2^{(1)} = \beta_1\omega_1(\Delta_1 - \Delta_2) + \psi_{1,2} + \phi_1 + \tilde{\phi}_2^{(1)} \tag{4}$$

where $\tilde{\omega}_2^{(1)}$ and $\tilde{\phi}_2^{(1)}$ are the frequency and phase estimation error, respectively, at BS_2 in $\mathsf{TS}^{(1)}$. Note that any nonrandom parameter estimation technique can be used to generate these estimates based on the observation $y_2^{(1)}(t_2)$, e.g., maximum likelihood (ML) estimation. A detailed description of single-tone ML parameter estimation can be found in [24].

This process is repeated through increasing base station indices. In each timeslot, a base station transmits a periodic extension of the beacon it received in the prior timeslot to the next base station (except for the

TABLE I
ESTIMATES AT EACH BASE STATION AFTER THE TWO-WAY BASE STATION SYNCHRONIZATION PROTOCOL

Base station	First phase estimate	First freq. estimate	Second phase estimate	Second freq. estimate
BS_1	$\hat{\phi}_{1,1} = \phi_1$	$\hat{\omega}_{1,1} = \omega_1$	$\hat{\phi}_{1,2} = \hat{\phi}_1^{(2M-2)}$	$\hat{\omega}_{1,2} = \hat{\omega}_1^{(2M-2)}$
BS_i, $i = 2, \ldots, M-1$	$\hat{\phi}_{i,1} = \hat{\phi}_i^{(i-1)}$	$\hat{\omega}_{i,1} = \hat{\omega}_i^{(i-1)}$	$\hat{\phi}_{i,2} = \hat{\phi}_i^{(2M-i-1)}$	$\hat{\omega}_{i,2} = \hat{\omega}_i^{(2M-i-1)}$
BS_M	$\hat{\phi}_{M,1} = \hat{\phi}_M^{(M-1)}$	$\hat{\omega}_{M,1} = \hat{\omega}_M^{(M-1)}$	$\hat{\phi}_{M,2} = \phi_M$	$\hat{\omega}_{M,2} = \omega_M$

magnitude, which is set to one for each transmission). The signal transmitted by BS_{i-1} to BS_i in $\mathsf{TS}^{(i-1)}$ is $x_{i-1}^{(i-1)}(t_{i-1}) = \exp\{j(\hat{\omega}_{i-1}^{(i-2)} t_{i-1} + \hat{\phi}_{i-1}^{(i-2)})\}\mathbb{I}_{t_{i-1} \in T_{i-1}^{(i-1)}}$. After propagation through the LTI channel to BS_i, the signal is received as

$$y_i^{(i-1)}(t_i) = a_{i-1,i} \exp\left\{ j \left(\beta_{i-1} \hat{\omega}_{i-1}^{(i-2)} \left(\frac{t_i}{\beta_i} + \Delta_{i-1} - \Delta_i \right) + \psi_{i-1,i} + \hat{\phi}_{i-1}^{(i-2)} \right) \right\} \mathbb{I}_{t_i \in T_i^{(i-1)}} + w_i^{(i-1)}(t_i).$$

This observation is then used by BS_i to generate frequency and phase estimates

$$\hat{\omega}_i^{(i-1)} = \frac{\beta_{i-1} \hat{\omega}_{i-1}^{(i-2)} + \tilde{\omega}_i^{(i-1)}}{\beta_i}, \text{and} \tag{5}$$

$$\hat{\phi}_i^{(i-1)} = \beta_{i-1} \hat{\omega}_{i-1}^{(i-2)} (\Delta_{i-1} - \Delta_i) + \psi_{i-1,i} + \hat{\phi}_{i-1}^{(i-2)} + \tilde{\phi}_i^{(i-1)} \tag{6}$$

for $i = 3, \ldots, M$, where $\tilde{\omega}_i^{(i-1)}$ and $\tilde{\phi}_i^{(i-1)}$ are the frequency and phase estimation error, respectively, at BS_i in $\mathsf{TS}^{(i-1)}$. The forward propagation stage concludes at the end of $\mathsf{TS}^{(M-1)}$.

Backward propagation is the same as forward propagation except BS_M initiates the process by transmitting a sinusoidal beacon $x_M^{(M)}(t_M) = \exp\{j(\omega_M t_M + \phi_M)\}\mathbb{I}_{t_M \in T_M^{(M)}}$ to BS_{M-1}. The beacons are retransmitted through decreasing base station indices $i = M-1, \ldots, 1$ and the backward propagation stage concludes after BS_1 receives the final beacon in $\mathsf{TS}^{(2M-2)}$.

At the end of the of two-way base station synchronization protocol, each base station has two sets of phase and frequency estimates as shown in Table I. Note that BS_1 and BS_M actually each have only one set of phase and frequency estimates; the initial beacon phase and frequency (ω_1 and ϕ_1 or ω_M and ϕ_M) are used as the other "estimates".

Before describing how the estimates in Table I can be used to synchronize the base stations' carriers, we make two remarks regarding practical implementation of the two-way synchronization protocol:

1) The two-way carrier synchronization protocol requires the base stations to receive and retransmit synchronization beacons according to the established base station ordering. Under our assumption that the synchronization beacons are exchanged wirelessly among the base stations, a practical implementation of the protocol would likely require some mechanism to avoid erroneous reception and retransmission of a beacon by a base station. This could be achieved in a variety of ways including modulating a portion of each beacon with originator and/or recipient information, backhaul signaling to notify base stations when to listen for a beacon, and/or the establishment of a fixed synchronization timeslot schedule so that base stations know which beacons to ignore and which to receive based upon their time of arrival.
2) Under our assumption that the synchronization beacons are exchanged wirelessly among the base stations, each base station could potentially form a larger table of phase and frequency estimates if it did not ignore the synchronization beacons from the nonpreceding and nonsubsequent base stations in the ordering. As shown in the following section, however, these additional beacon observations are not necessary to synchronize the base stations' carriers. Estimating the phase and frequency of additional beacon observations in the forward and backward propagation stages does not affect the resulting synchronized local oscillator *phase* but could improve the accuracy of the synchronized local oscillator *frequency* through techniques such as maximal ratio combining.

A. Synthesizing Synchronized Local Oscillators From Local Estimates

After BS_i forms estimates of the phase and frequency of the beacons it received in the forward and backward propagation stages, it synthesizes a "synchronized local oscillator" (SLO)

$$v_i(t_i) = \exp\{j(\hat{\omega}_i t_i + \hat{\phi}_i)\} \tag{7}$$

where $\hat{\omega}_i = \hat{\omega}_{i,1} + \hat{\omega}_{i,2}$ and $\hat{\phi}_i = \hat{\phi}_{i,1} + \hat{\phi}_{i,2}$ are the SLO frequency and phase, respectively, generated by adding the frequency and phase estimates from the forward and backward propagation stages. If we temporarily assume that the estimates at BS_i are perfect[2] in the sense that there is no estimation error, it is not difficult to show that the SLO at BS_i has the same frequency and phase (modulo 2π) as the other base stations. To see this, we can use (5) in the forward propagation stage to write the first frequency estimate at BS_i as

$$\hat{\omega}_{i,1} = \frac{\beta_{i-1}}{\beta_i} \hat{\omega}_{i-1,1} = \frac{\beta_1}{\beta_i} \omega_1$$

for $i = 2, \ldots, M$. The second equality results from a recursive application of the first equality and the fact that $\hat{\omega}_{1,1} := \omega_1$. Along the same lines, we can use (5) in the backward propagation stage to write the second frequency estimate at BS_i as

$$\hat{\omega}_{i,2} = \frac{\beta_{i+1}}{\beta_i} \hat{\omega}_{i+1,2} = \frac{\beta_M}{\beta_i} \omega_M$$

[2]Imperfect estimates are considered in Section IV.

for $i = M-1, \ldots, 1$ where $\hat{\omega}_{M,2} := \omega_M$. The resulting SLO frequency at BS_i is then

$$\hat{\omega}_i = \hat{\omega}_{i,1} + \hat{\omega}_{i,2} = \frac{\beta_1\omega_1 + \beta_M\omega_M}{\beta_i}. \quad (8)$$

The first phase estimate at BS_i can be calculated from (5) and (6) in the forward propagation stage as

$$\begin{aligned}\hat{\phi}_{i,1} &= (\beta_1\omega_1(\Delta_{i-1} - \Delta_i) \\ &\quad + \psi_{i-1,i} + \hat{\phi}_{i-1,1}) \pmod{2\pi} \\ &= \left(\beta_1\omega_1(\Delta_1 - \Delta_i) \right. \\ &\quad \left. + \sum_{\ell=1}^{i-1}\psi_{\ell,\ell+1} + \phi_1\right) \pmod{2\pi}\end{aligned}$$

for $i = 2, \ldots, M$ where we have used $\beta_{i-1}\hat{\omega}_{i-1}^{(i-2)} = \beta_{i-1}\hat{\omega}_{i-1,1} = \beta_1\omega_1$ and where the second equality results from a recursive application of the first equality. Note that the unavoidable 2π periodic ambiguity in the phase estimates is represented here by the modulo operation. Along the same lines, we can use (5) and (6) in the backward propagation stage to write the second phase estimate at BS_i as

$$\begin{aligned}\hat{\phi}_{i,2} &= (\beta_M\omega_M(\Delta_{i+1} - \Delta_i) \\ &\quad + \psi_{i+1,i} + \hat{\phi}_{i+1,2}) \pmod{2\pi} \\ &= \left(\beta_M\omega_M(\Delta_M - \Delta_i) \right. \\ &\quad \left. + \sum_{\ell=i}^{M-1}\psi_{\ell+1,\ell} + \phi_M\right) \pmod{2\pi}\end{aligned}$$

for $i = M-1, \ldots, 1$. Assuming forward and backward propagation frequencies are close such that channel reciprocity holds and $\psi_{\ell+1,\ell} = \psi_{\ell,\ell+1}$, the resulting SLO phase at BS_i is then

$$\begin{aligned}\hat{\phi}_i &= \left(\hat{\phi}_{i,1} + \hat{\phi}_{i,2}\right) \pmod{2\pi} \\ &= (\beta_1\omega_1(\Delta_1 - \Delta_i) + \beta_M\omega_M \\ &\quad \times (\Delta_M - \Delta_i) + \bar{\psi} + \phi_1 + \phi_M) \pmod{2\pi} \quad (9)\end{aligned}$$

where, for notational convenience, we have defined $\bar{\psi} := \sum_{\ell=1}^{M-1}\psi_{\ell,\ell+1}$.

Putting it all together, we can plug (8) and (9) into (7) to write

$$\begin{aligned}v_i(t_i) = \exp\left\{j\left(\frac{\beta_1\omega_1 + \beta_M\omega_M}{\beta_i}t_i + \beta_1\omega_1(\Delta_1 - \Delta_i)\right.\right. \\ \left.\left. + \beta_M\omega_M(\Delta_M - \Delta_i) + \bar{\psi} + \phi_1 + \phi_M\right)\right\} \quad (10)\end{aligned}$$

where we have dropped the modulo since it does not affect the expression. Using (2), we can rewrite (10) in reference time as

$$v_i(t) = \exp\left\{j\left((\beta_1\omega_1 + \beta_M\omega_M)t + \gamma_1 + \gamma_M + \bar{\psi}\right)\right\} \quad (11)$$

where $\gamma_m := \beta_m\omega_m\Delta_m + \phi_m$. Note that this last expression is not a function of i. Hence, even though BS_i possesses its own local notion of time and operates only on its own local estimates, the SLO frequency at BS_i is identical and the SLO phase at each base station is identical (modulo 2π) to the other base stations in the network after two-way carrier synchronization.

B. A Didactic Example

While the previous section presented a general analysis showing that all of the base stations in the cellular network can form synchronized local oscillators by following the two-way synchronization protocol, we present here a simple example in order to illustrate the main idea behind the technique. We consider a scenario with $M = 2$ base stations with a fixed clock offset and no clock rate offset, i.e., $\Delta_1 \neq \Delta_2$ and $\beta_1 = \beta_2$. There are only two timeslots in this case. By following the two-way synchronization protocol, we will show explicitly that BS_1 and BS_2 are able to form synchronized local oscillators with identical phase and frequency in the absence of estimation error.

In $\mathsf{TS}^{(1)}$, BS_1 transmits a beacon to BS_2 and BS_2 estimates the frequency and phase of this beacon as

$$\begin{aligned}&\hat{\omega}_{2,1} = \omega_1 \text{ and} \\ &\hat{\phi}_{2,1} = (\omega_1(\Delta_1 - \Delta_2) + \psi_{1,2} + \phi_1) \pmod{2\pi}.\end{aligned}$$

In $\mathsf{TS}^{(2)}$, BS_2 transmits a beacon to BS_1 and BS_1 estimates the frequency and phase of this beacon as

$$\begin{aligned}&\hat{\omega}_{1,2} = \omega_2 \text{ and} \\ &\hat{\phi}_{1,2} = (\omega_2(\Delta_2 - \Delta_1) + \psi_{2,1} + \phi_2) \pmod{2\pi}.\end{aligned}$$

After the beacons are exchanged, BS_1 generates its SLO by summing the frequency and phase of the local carrier (ω_1 and ϕ_1) with its frequency and phase estimates in $\mathsf{TS}^{(2)}$ ($\hat{\omega}_{1,2}$ and $\hat{\phi}_{1,2}$). The SLO at BS_1 in the local timebase of BS_1 is then

$$\begin{aligned}v_1(t_1) = \exp\left\{j\underbrace{(\omega_1 t_1 + \phi_1)}_{\text{local carrier at } \mathsf{BS}_1}\right. \\ \left. + j\underbrace{(\omega_2 t_1 + \omega_2(\Delta_2 - \Delta_1) + \psi_{2,1} + \phi_2)}_{\text{estimated carrier from } \mathsf{BS}_2}\right\}\end{aligned}$$

where the $\pmod{2\pi}$ is dropped since it doesn't affect the expression. After substituting $t_1 = t + \Delta_1$ and simplifying, we get the SLO at BS_1 in reference time as

$$\begin{aligned}v_1(t) = \exp\{j((\omega_1 + \omega_2)t + \omega_1\Delta_1 \\ + \omega_2\Delta_2 + \phi_1 + \phi_2 + \psi_{2,1})\}.\end{aligned}$$

BS_2 generates its SLO similarly. The SLO at BS_2 in the local timebase of BS_2 is formed as

$$\begin{aligned}v_2(t_2) = \exp\left\{j\underbrace{(\omega_2 t_2 + \phi_2)}_{\text{local carrier at } \mathsf{BS}_2}\right. \\ \left. + j\underbrace{(\omega_1 t_2 + \omega_1(\Delta_1 - \Delta_2) + \psi_{1,2} + \phi_1)}_{\text{estimated carrier from } \mathsf{BS}_1}\right\}.\end{aligned}$$

After substituting $t_2 = t + \Delta_2$ and simplifying, we get the SLO at BS_2 in reference time as

$$v_2(t) = \exp\{j((\omega_1 + \omega_2)t + \omega_1\Delta_1 + \omega_2\Delta_2 + \phi_1 + \phi_2 + \psi_{1,2})\}.$$

It is clear that $v_1(t) = v_2(t)$ when channel reciprocity holds, i.e., if $\psi_{1,2} = \psi_{2,1}$.

Frequency synchronization of the SLOs via two-way synchronization is easy to understand intuitively. Each base station observes a beacon during forward propagation and another beacon during backward propagation (the first and last base stations use their local carriers as a proxy for these observations as shown in the example above). The SLO frequency is simply the sum of the two frequency estimates. If the estimation errors are not too large (as discussed in Section IV), all of the base stations will have approximately identical estimates and hence will form SLOs with synchronized frequencies.

Phase synchronization of the SLOs via two-way synchronization is less straightforward than frequency synchronization but can be intuitively explained as follows. During forward propagation, BS_m observes the original beacon from BS_1 with an accumulated phase shift of $\psi_{1,2} + \cdots + \psi_{m-1,m}$ since each base station retransmits a periodic extension of the signal it received in the previous timeslot. During backward propagation, BS_m observes the original beacon from BS_M with an accumulated phase shift of $\psi_{M,M-1} + \cdots + \psi_{m+1,m}$. These two phases are then summed to form the SLO phase. If the estimation errors are not too large and if channel reciprocity holds, then each base station will have the same SLO phase since the SLO phase

$$\underbrace{\psi_{1,2} + \cdots + \psi_{m-1,m}}_{\text{forward phase}} + \underbrace{\psi_{M,M-1} + \cdots + \psi_{m+1,m}}_{\text{backward phase}} = \sum_{i=1}^{M-1} \psi_{i,i+1}$$

is not a function of m.

C. Multicell Retrodirective Downlink Beamforming

After two-way synchronization has been performed among the M base stations in the cellular network, the base stations listen for an uplink transmission from a mobile in the network. For simplicity, we assume that the uplink/downlink signals are narrowband, single-carrier, and TDD. Although not discussed here, the two-way synchronization technique can also be used to facilitate distributed beamforming in frequency division duplex (FDD) channels using techniques such as those described in [25] and [26].

In the TDD uplink channel, the mobile transmits the uplink signal $x_0^{(\mathsf{up})}(t_0) = \exp\{j(\omega_0 t_0 + \phi_0)\}\mathbb{I}_{t_0 \in T_0^{(\mathsf{up})}}$ (possibly modulated by a message signal not shown here for clarity) on the interval $T_0^{(\mathsf{up})}$ and this signal is received by a subset $\mathcal{M}_0 \subseteq \{1, \ldots, M\}$ of the base stations in the network. It is assumed these base stations all have a copy of the downlink message to be sent to the mobile, distributed by the MSC via the cellular network backhaul. The mobile's uplink transmission is received at BS_i on the interval $T_i^{(\mathsf{up})}$ as

$$\begin{aligned} y_i^{(\mathsf{up})}(t_i) &= a_{0,i} \exp\left\{ j\left(\beta_0\omega_0 \left(\frac{t_i}{\beta_i} + \Delta_0 - \Delta_i \right) + \psi_{0,i} + \phi_0 \right) \right\} \\ &\quad \times \mathbb{I}_{t_i \in T_i^{(\mathsf{up})}} + w_i^{(\mathsf{up})}(t_i) \end{aligned}$$

in local time for all $i \in \mathcal{M}_0$ with $a_{0,i} = |G_{0,i}(\beta_0\omega_0)|$ and $\psi_{0,i} = \angle G_{0,i}(\beta_0\omega_0)$. The term $w_i^{(\mathsf{up})}(t_i)$ is the uplink signal observation noise at BS_i. From this observation, BS_i forms the local phase estimate

$$\hat{\omega}_i^{(\mathsf{up})} = \frac{\beta_0\omega_0 + \tilde{\omega}_i^{(\mathsf{up})}}{\beta_i}, \text{ and} \tag{12}$$

$$\hat{\phi}_i^{(\mathsf{up})} = \beta_0\omega_0(\Delta_0 - \Delta_i) + \psi_{0,i} + \phi_0 + \tilde{\phi}_i^{(\mathsf{up})} \tag{13}$$

where $\tilde{\omega}_i^{(\mathsf{up})}$ and $\tilde{\phi}_i^{(\mathsf{up})}$ are the frequency and phase estimation error, respectively, at BS_i from observation of the mobile's uplink transmission.

At BS_i, the downlink carrier is generated using the local estimates in (12) and (13), together with the frequency and phase of the SLO in (8) and (9), according to

$$x_i^{(\mathsf{down})}(t_i) = \exp\left\{ j\left((\hat{\omega}_i - \hat{\omega}_i^{(\mathsf{up})})t_i + \hat{\phi}_i - \hat{\phi}_i^{(\mathsf{up})} \right) \right\}. \tag{14}$$

Defining $\bar{\gamma} := \gamma_1 + \gamma_M - \gamma_0$, we can use (2) to rewrite (14) in reference time as

$$\begin{aligned} x_i^{(\mathsf{down})}(t) &= \exp\left\{ j\left(\left(\hat{\omega}_i - \hat{\omega}_i^{(\mathsf{up})} \right) \times (\beta_i(t + \Delta_i)) + \hat{\phi}_i - \hat{\phi}_i^{(\mathsf{up})} \right) \right\} \mathbb{I}_{t \in T_i^{(\mathsf{down})}} \\ &= \exp\{j((\beta_1\omega_1 + \beta_M\omega_M - \beta_0\omega_0)t + \bar{\gamma} + \bar{\psi} - \psi_{0,i})\} \mathbb{I}_{t \in T_i^{(\mathsf{down})}} \end{aligned}$$

for all $i \in \mathcal{M}_0$ on the interval $T_i^{(\mathsf{down})}$, where we have again assumed the frequency and phase estimation errors are all zero to ease exposition. After downlink propagation, the aggregate signal at the mobile (in reference time) can be written as

$$\begin{aligned} y_0^{(\mathsf{down})}(t) &= \sum_{i \in \mathcal{M}_0} a_{i,0} \exp\{j((\beta_1\omega_1 + \beta_M\omega_M - \beta_0\omega_0)t + \bar{\gamma} + \bar{\psi} - \psi_{0,i} + \psi_{i,0})\} \\ &\quad \times \mathbb{I}_{t \in T_{i,0}^{(\mathsf{down})}} + w_0^{(\mathsf{down})}(t) \end{aligned}$$

where $T_{i,0}^{(\mathsf{down})}$ is the interval the signal transmitted by BS_i is received at the mobile, $a_{i,0} = |G_{i,0}(\beta_1\omega_1 + \beta_M\omega_M - \beta_0\omega_0)|$, and $\psi_{i,0} = \angle G_{i,0}(\beta_1\omega_1 + \beta_M\omega_M - \beta_0\omega_0)$. Channel reciprocity occurs in TDD operation when the uplink and downlink frequencies are (at least approximately) identical, which is achieved here when $\beta_1\omega_1 + \beta_M\omega_M \approx 2\beta_0\omega_0$. When this condition holds,

then $\psi_{i,0} = \psi_{0,i}$, $a_{i,0} = a_{0,i}$, and the aggregate signal at the mobile can be written as

$$y_0^{(\mathsf{down})}(t) = \sum_{i\in\mathcal{M}_0} a_{0,i}\exp\{j((\beta_1\omega_1+\beta_M\omega_M-\beta_0\omega_0)t+\bar{\gamma}+\bar{\psi})\} \times \mathbb{I}_{t\in T_{i,0}^{(\mathsf{down})}} + w_0^{(\mathsf{down})}(t).$$

Assuming the baseband signals are synchronized to a small fraction of the symbol period[3], the received power of the aggregate signal at the mobile in this case is $|y_0^{(\mathsf{down})}(t)|^2 = \left(\sum_{i\in\mathcal{M}_0} a_{0,i}\right)^2$. This corresponds to the power of an "ideal" downlink beamformer when each base station transmits with unit downlink carrier amplitude.

While the preceding analysis was based on a single-carrier TDD uplink/downlink, retrodirective transmission can be extended to multicarrier TDD systems by having the mobile to transmit a multicarrier uplink signal and having each base station form local phase and frequency estimates of each subcarrier. The estimates in (12) and (13) would then be indexed by both base station and subcarrier, and the downlink transmission in (14) would instead be a multicarrier signal with phase and frequency estimates applied to facilitate retrodirective transmission on a subcarrier-by-subcarrier basis.

For clarity of exposition, we also note that the preceding analysis was based on the implicit assumption that the mobile was stationary or slowly moving such that the uplink and downlink channels are reciprocal during the uplink beacon transmission and subsequent downlink beamforming. This assumption may not be valid in systems with long beamforming times, high carrier frequencies, and/or high node mobility. In these cases, one solution is to have the mobile transmit more frequent uplink beacons to maintain uplink/downlink channel reciprocity and retrodirectivity. A more efficient approach is to use retrodirective tracking techniques to automatically steer the beam along the path of the mobile as described in [28]. In any case, node mobility only affects retrodirectivity; the two-way synchronization protocol is unmodified by node mobility since the base stations are stationary.

IV. Performance Analysis of MultiCell Retrodirective Downlink Beamforming

Estimation errors incurred during two-way synchronization and downlink channel estimation as well as phase noise at each base station all lead to some loss of performance with respect to the ideal downlink beamformer power prediction. At time t, the power of the aggregate received signal from the set of base stations $\mathcal{M}_0$ at the mobile can be expressed as

$$\left|y_0^{(\mathsf{down})}(t)\right|^2 = \sum_{m\in\mathcal{M}_0} a_{0,m}^2 + \sum_{m\in\mathcal{M}_0}\sum_{\substack{n\in\mathcal{M}_0\\ n\neq m}} a_{0,m}a_{0,n}\cos(\delta_{m,n}(t)) \quad (15)$$

where the nonideal nature of the distributed beamformer is captured in the pairwise carrier offset terms

$$\begin{aligned}\delta_{m,n}(t) := &\left(\hat{\omega}_m - \hat{\omega}_m^{(\mathsf{up})}\right)\beta_m(t+\Delta_m) - \left(\hat{\omega}_n - \hat{\omega}_n^{(\mathsf{up})}\right)\beta_n(t+\Delta_n)\\ &+ \left(\hat{\phi}_m - \hat{\phi}_m^{(\mathsf{up})} + \psi_{m,0}\right) - \left(\hat{\phi}_n - \hat{\phi}_n^{(\mathsf{up})} + \psi_{n,0}\right) + \chi_m(t) - \chi_n(t) \quad (16)\end{aligned}$$

between BS_m and BS_n and where $\chi_m(t) - \chi_n(t)$ represents the difference in the phase noise processes of the SLOs between BS_m and BS_n. Note that (16) is composed of three components: pairwise carrier frequency offset, pairwise initial carrier phase offset at $t = 0$, and pairwise phase noise offset. We can rewrite (16) in these terms as

$$\delta_{m,n}(t) = \tilde{\omega}_{m,n}(t) + \tilde{\phi}_{m,n} + \chi_m(t) - \chi_n(t). \quad (17)$$

From (8), (9), (12), and (13), we can write the frequency[4] and phase estimates as

$$\hat{\omega}_m = \frac{\beta_1\omega_1 + \beta_M\omega_M + \tilde{\omega}_m}{\beta_m}, \quad (18)$$

$$\hat{\omega}_m^{(\mathsf{up})} = \frac{\beta_0\omega_0 + \tilde{\omega}_m^{(\mathsf{up})}}{\beta_m}, \quad (19)$$

$$\hat{\phi}_m = \beta_1\omega_1(\Delta_1-\Delta_m) + \beta_M\omega_M(\Delta_M-\Delta_m) + \phi_1 + \phi_M + \bar{\psi} + \tilde{\phi}_m, \quad \text{and} \quad (20)$$

$$\hat{\phi}_m^{(\mathsf{up})} = \beta_0\omega_0(\Delta_0-\Delta_m) + \psi_{0,m} + \phi_0 + \tilde{\phi}_m^{(\mathsf{up})} \quad (21)$$

where $\tilde{\omega}_m$ and $\tilde{\phi}_m$ are the frequency and phase errors, respectively, of the SLO generated according to the procedure in Section III.A. These results can be combined to write the pairwise frequency and phase offsets in (17) as

$$\tilde{\omega}_{m,n} = (\tilde{\omega}_m - \tilde{\omega}_m^{(\mathsf{up})}) - (\tilde{\omega}_n - \tilde{\omega}_n^{(\mathsf{up})}), \quad (22)$$

$$\tilde{\phi}_{m,n} = (\tilde{\phi}_m - \tilde{\phi}_m^{(\mathsf{up})}) - (\tilde{\phi}_n - \tilde{\phi}_n^{(\mathsf{up})}) + \Delta_m\left(\tilde{\omega}_m - \tilde{\omega}_m^{(\mathsf{up})}\right) - \Delta_n(\tilde{\omega}_n - \tilde{\omega}_n^{(\mathsf{up})}) \quad (23)$$

To facilitate an analysis of the relationship between the pairwise carrier and phase offsets in (22) and (23) and the constituent estimation errors $\{\tilde{\omega}_m^{(m-1)}, \tilde{\omega}_m^{(2M-m-1)}, \tilde{\phi}_m^{(m-1)}, \tilde{\phi}_m^{(2M-m-1)}, \tilde{\omega}_m^{(\mathsf{up})}, \tilde{\phi}_m^{(\mathsf{up})}\}$ for $m = 1,\ldots,M$, we define the constituent estimation error vectors

$$\tilde{\boldsymbol{\theta}}_\omega := \left[0, \tilde{\omega}_2^{(1)}, \ldots, \tilde{\omega}_M^{(M-1)}, \tilde{\omega}_1^{(2M-2)}, \ldots, \tilde{\omega}_{M-1}^{(M)}, 0\right]^\top \in \mathbb{R}^{2M\times 1} \quad (24)$$

$$\tilde{\boldsymbol{\theta}}_\phi := \left[0, \tilde{\phi}_2^{(1)}, \ldots, \tilde{\phi}_M^{(M-1)}, \tilde{\phi}_1^{(2M-2)}, \ldots, \tilde{\phi}_{M-1}^{(M)}, 0\right]^\top \in \mathbb{R}^{2M\times 1} \quad (25)$$

[3]The timing accuracy requirements for symbol alignment can usually be satisfied with conventional synchronization techniques, e.g., GPS or IEEE 1588 [27], and the deleterious effects of symbol offset, i.e., intersymbol interference, can be mitigated through baseband signal processing techniques such as channel equalization.

[4]The analysis in this section assumes the base stations strictly follow the two-way synchronization protocol as described in Section III. Since each base station uses only the beacon observations from the preceding and subsequent base stations to calculate its SLO frequency, these results can be considered a conservative performance prediction.

$$\tilde{\boldsymbol{\theta}}_{\omega}^{(\mathsf{up})} := \left[\tilde{\omega}_1^{(\mathsf{up})}, \ldots, \tilde{\omega}_M^{(\mathsf{up})}\right]^{\top} \in \mathbb{R}^{M\times 1} \tag{26}$$

$$\tilde{\boldsymbol{\theta}}_{\phi}^{(\mathsf{up})} := \left[\tilde{\phi}_1^{(\mathsf{up})}, \ldots, \tilde{\phi}_M^{(\mathsf{up})}\right]^{\top} \in \mathbb{R}^{M\times 1}. \tag{27}$$

Note the zeros in the first and last positions of both $\tilde{\boldsymbol{\theta}}_{\omega}$ and $\tilde{\boldsymbol{\theta}}_{\phi}$. These zeros result from the fact that BS_1 and BS_M have no estimation error with respect to the beacons each transmits at the start of the forward and backward propagation stages, respectively. As will be shown in the sequel, these zeros also allow for a more straightforward representation of the relationship between the constituent estimation errors and the pairwise carrier offset terms in (22) and (23).

A. Pairwise Carrier Frequency Offset

In the forward propagation stage of the two-way base station synchronization protocol, the estimation error $\tilde{\omega}_i^{(i-1)}$ in (5) is defined with respect to the true frequency of the signal transmitted by BS_{i-1} in $\mathsf{TS}^{(i-1)}$. In $\mathsf{TS}^{(1)}$, the true frequency of transmission is $\beta_1\omega_1$. In $\mathsf{TS}^{(i-1)}$ for $i = 3, \ldots, M$, the true frequency of transmission is $\beta_{i-1}\hat{\omega}_{i-1}^{(i-2)}$. The serial nature of the transmissions in the two-way base station synchronization protocol implies that the frequency error at BS_i with respect to the initial true beacon frequency $\beta_1\omega_1$ is an accumulation of the individual frequency estimation errors, i.e., $\tilde{\omega}_2^{(1)} + \ldots + \tilde{\omega}_i^{(i-1)}$. The same is true for the backward propagation stage except the true frequency of the initial beacon is $\beta_M\omega_M$.

The frequency error of the SLO at BS_i can be computed from (18) and recursive application of (5) for the forward and backward propagation stages as

$$\tilde{\omega}_i = \sum_{\ell=2}^{i} \tilde{\omega}_{\ell}^{(\ell-1)} + \sum_{\ell=i}^{M-1} \tilde{\omega}_{\ell}^{(2M-\ell-1)} \tag{28}$$

where the first and second sums correspond to the accumulated estimation error at BS_i in the forward and backward propagation stages, respectively. Defining $\tilde{\boldsymbol{\omega}} := [\tilde{\omega}_1, \ldots, \tilde{\omega}_M]^{\top}$ we can compactly express (28) for $i = 1, \ldots, M$ as

$$\tilde{\boldsymbol{\omega}} = [\boldsymbol{U}^{\top}, \boldsymbol{U}]\tilde{\boldsymbol{\theta}}_{\omega} = \boldsymbol{A}\tilde{\boldsymbol{\theta}}_{\omega} \tag{29}$$

where $\boldsymbol{U} \in \mathbb{R}^{M\times M}$ is an upper triangular matrix defined by

$$\boldsymbol{U}_{ij} = \begin{cases} 1 & i \geq j \\ 0 & \text{otherwise} \end{cases}$$

for $i = 1, \ldots, m$ and $j = 1, \ldots, m$, $\boldsymbol{A} \in \mathbb{R}^{M\times 2M}$, and $\tilde{\boldsymbol{\theta}}_{\omega}$ is defined in (24).

After synchronization, the mobile broadcasts a beacon to the base stations. BS_m then generates a local frequency estimate $\hat{\omega}_m^{(\mathsf{up})}$ and subtracts this estimate from the SLO frequency estimate $\hat{\omega}_m$. The resulting pairwise carrier frequency offset in (22) between BS_m and BS_n can then be written as

$$\tilde{\omega}_{m,n} = (\boldsymbol{e}_m - \boldsymbol{e}_n)^{\top}\left[\boldsymbol{A}\tilde{\boldsymbol{\theta}}_{\omega} - \tilde{\boldsymbol{\theta}}_{\omega}^{(\mathsf{up})}\right] \tag{30}$$

where $\boldsymbol{e}_i$ is the ith standard basis column vector and $\tilde{\boldsymbol{\theta}}_{\omega}^{(\mathsf{up})}$ is defined in (26).

B. Pairwise Carrier Phase Offset

Similar to the frequency estimation errors, the phase estimation errors in the forward and backward propagation stages of the two-way base station synchronization protocol accumulate as the signals propagate through increasing and decreasing base station indices. The accumulation of phase error at BS_i, however, is due to both constituent phase and frequency estimation errors. In the forward propagation stage of the two-way synchronization protocol, we can recursively apply (5) and (6) to write the first local phase estimate at BS_i as

$$\begin{aligned}\hat{\phi}_{i,1} &= \hat{\phi}_i^{(i-1)} \\ &= \beta_1\omega_1(\Delta_1 - \Delta_i) + \phi_1 + \sum_{\ell=2}^{i}\psi_{\ell-1,\ell} \\ &\quad + \sum_{\ell=2}^{i}\tilde{\phi}_{\ell}^{(\ell-1)} + \sum_{\ell=2}^{i-1}\tilde{\omega}_{\ell}^{(\ell-1)}(\Delta_{\ell} - \Delta_i)\end{aligned}$$

for $i = 2, \ldots, M$. Similarly, we can write the second local phase estimate at BS_i as

$$\begin{aligned}\hat{\phi}_{i,2} &= \hat{\phi}_i^{(2M-i-1)} \\ &= \beta_M\omega_M(\Delta_M - \Delta_i) + \phi_M + \sum_{\ell=i}^{M-1}\psi_{\ell,\ell+1} \\ &\quad + \sum_{\ell=i}^{M-1}\tilde{\phi}_{\ell}^{(2M-\ell-1)} + \sum_{\ell=i+1}^{M-1}\tilde{\omega}_{\ell}^{(2M-\ell-1)}(\Delta_{\ell} - \Delta_i)\end{aligned}$$

for $i = 1, \ldots, M-1$. These estimates are summed at BS_i and the resulting phase error is

$$\begin{aligned}\tilde{\phi}_i &= \sum_{\ell=2}^{i}\tilde{\phi}_{\ell}^{(\ell-1)} + \sum_{\ell=2}^{i-1}\tilde{\omega}_{\ell}^{(\ell-1)}(\Delta_{\ell} - \Delta_i) \\ &\quad + \sum_{\ell=i}^{M-1}\tilde{\phi}_{\ell}^{(2M-\ell-1)} + \sum_{\ell=i+1}^{M-1}\tilde{\omega}_{\ell}^{(2M-\ell-1)}(\Delta_{\ell} - \Delta_i).\end{aligned} \tag{31}$$

Defining $\tilde{\boldsymbol{\phi}} := [\tilde{\phi}_1, \ldots, \tilde{\phi}_M]^{\top}$ we can compactly express (31) for $i = 1, \ldots, M$ as

$$\tilde{\boldsymbol{\phi}} = [-\boldsymbol{D}^{\top}, \boldsymbol{D}]\tilde{\boldsymbol{\theta}}_{\omega} + [\boldsymbol{U}^{\top}, \boldsymbol{U}]\tilde{\boldsymbol{\theta}}_{\phi} = \boldsymbol{B}\tilde{\boldsymbol{\theta}}_{\omega} + \boldsymbol{A}\tilde{\boldsymbol{\theta}}_{\phi} \tag{32}$$

where $\boldsymbol{B} \in \mathbb{R}^{M\times 2M}$, $\boldsymbol{U}$ and $\boldsymbol{A}$ are defined in (29), $\tilde{\boldsymbol{\theta}}_{\omega}$ and $\tilde{\boldsymbol{\theta}}_{\phi}$ are defined in (24) and (25), respectively, and $\boldsymbol{D} \in \mathbb{R}^{M\times M}$ is a strictly upper triangular matrix defined by

$$\boldsymbol{D}_{ij} = \begin{cases} \Delta_i - \Delta_j & i > j \\ 0 & \text{otherwise} \end{cases}$$

for $i = 1, \ldots, m$ and $j = 1, \ldots, m$. Note that $\boldsymbol{D} \in \mathbb{R}^{M\times M}$ is upper triangular with $\mathrm{diag}(\boldsymbol{D}) = [0, \ldots, 0]^{\top}$. After synchronization, the mobile broadcasts a beacon to the base stations. BS_m forms a local phase estimate $\hat{\phi}_m^{(\mathsf{up})}$ and subtracts this estimate from the estimated synchronization phase $\hat{\phi}_m$. The resulting pairwise carrier phase offset in (23) at time $t = 0$ between BS_m and BS_n can then be expressed as

$$\tilde{\phi}_{m,n} = (\boldsymbol{e}_m - \boldsymbol{e}_n)^{\top}\left(\tilde{\boldsymbol{\phi}} - \tilde{\boldsymbol{\theta}}_{\phi}^{(\mathsf{up})} + \boldsymbol{\Lambda}\left(\tilde{\boldsymbol{\omega}} - \tilde{\boldsymbol{\theta}}_{\omega}^{(\mathsf{up})}\right)\right) \tag{33}$$

$$= (\boldsymbol{e}_m - \boldsymbol{e}_n)^\top \left[(\boldsymbol{B} + \boldsymbol{\Lambda}\boldsymbol{A})\tilde{\boldsymbol{\theta}}_\omega + \boldsymbol{A}\tilde{\boldsymbol{\theta}}_\phi - \boldsymbol{\Lambda}\tilde{\boldsymbol{\theta}}_\omega^{(\mathsf{up})} - \tilde{\boldsymbol{\theta}}_\phi^{(\mathsf{up})} \right] \tag{34}$$

where $\boldsymbol{\Lambda} := \mathrm{diag}(\Delta_1, \ldots, \Delta_M)$, $\boldsymbol{e}_i$ is the ith standard basis column vector, and $\tilde{\boldsymbol{\theta}}_\phi^{(\mathsf{up})}$ is defined in (27).

C. Pairwise Phase Noise Offset

In addition to the pairwise phase and frequency offsets that occur as a consequence of imperfect estimation, practical oscillators also exhibit phase noise. Phase noise causes the phase of the SLO at each base station to randomly wander from the phase obtained at the end of the two-way synchronization protocol. As shown in [15], this can establish a ceiling on the reliable beamforming time even in the absence of estimation error.

The phase noise $\chi_i(t)$ at BS_i can be modeled as a zero-mean nonstationary Gaussian random process, independent of the estimation errors, with variance increasing linearly with time, i.e., $\sigma^2_{\chi_i}(t) = r(t - T_i^{\mathsf{sync}})$ for $t \geq T_i^{\mathsf{sync}}$, where T_i^{sync} is the time at which BS_i generates estimates $\hat{\omega}_i$ and $\hat{\phi}_i$. The variance parameter r is a function of the physical properties of the oscillator including its natural frequency and physical type [29]. We assume that all base stations share the same value of r but have independent phase noise processes. Using the procedure outlined in [30], a typical range of r for temperature compensated or oven controlled oscillators can be calculated as $0.005 \leq r \leq 0.1$ rad^2/sec for a nominal operating frequency of 1 GHz.

D. Overall Pairwise Carrier Offsets

Substituting (30) and (34) in (17), we can express the overall pairwise carrier offset between BS_m and BS_n in terms of the constituent estimation error vectors and phase noise processes as

$$\begin{aligned}\delta_{m,n}(t) = (\boldsymbol{e}_m - \boldsymbol{e}_n)^\top \Big\{ &[(\boldsymbol{I}t + \boldsymbol{\Lambda})\boldsymbol{A} + \boldsymbol{B}]\tilde{\boldsymbol{\theta}}_\omega \\ &+ \boldsymbol{A}\tilde{\boldsymbol{\theta}}_\phi - (\boldsymbol{I}t + \boldsymbol{\Lambda})\tilde{\boldsymbol{\theta}}_\omega^{(\mathsf{up})} - \tilde{\boldsymbol{\theta}}_\phi^{(\mathsf{up})} \Big\} \\ &+ \chi_m(t) - \chi_n(t). \end{aligned} \tag{35}$$

Note that, since $\delta_{m,n}(t)$ is a linear combination of the constituent estimation error vectors and the phase noise processes, the means and covariances of $\delta_{m,n}(t)$ can easily be expressed in terms of the means and covariances of the constituent error vectors and r. These expressions are simplified somewhat by the fact that the constituent error covariance matrices $\boldsymbol{\Theta}_{\omega\omega} := \mathrm{E}\{\tilde{\boldsymbol{\theta}}_\omega \tilde{\boldsymbol{\theta}}_\omega^\top\}$, $\boldsymbol{\Theta}_{\phi\phi}$, $\boldsymbol{\Theta}_{\omega\omega}^{(\mathsf{up})}$, and $\boldsymbol{\Theta}_{\phi\phi}^{(\mathsf{up})}$ (each defined similarly) are all diagonal since observations in different timeslots are affected by independent noise realizations and observations at different base stations are also affected by independent noise realizations. The other constituent error covariance matrices are all equal to zero except $\boldsymbol{\Theta}_{\omega\phi} := \mathrm{E}\{\tilde{\boldsymbol{\theta}}_\omega \tilde{\boldsymbol{\theta}}_\phi^\top\}$ and $\boldsymbol{\Theta}_{\omega\phi}^{(\mathsf{up})} := \mathrm{E}\{\tilde{\boldsymbol{\theta}}_\omega^{(\mathsf{up})} (\tilde{\boldsymbol{\theta}}_\phi^{(\mathsf{up})})^\top\}$ since frequency and phase estimates obtained from the same observation at a particular base station are not independent [24] in general.

V. Numerical Results

This section presents numerical examples of multicell retrodirective downlink beamforming in a system with M base stations using two-way synchronization. It is assumed in all of these examples that the phase/frequency estimator at each base station is unbiased and efficient with jointly Gaussian distributed estimation errors. Note that these are all asymptotic properties of the ML estimator under mild regularity conditions when the number of independent and identically distributed samples in the observation is large [31]. The covariance of the jointly Gaussian distributed constituent estimation errors at each base station is then given by the Cramer-Rao bound (CRB) [24]

$$\mathrm{cov}\{[\omega, \phi]^\top\} = \frac{\sigma^2}{a^2} \begin{bmatrix} \frac{1}{T_s^2 N_s (Q - P^2)} & \frac{-(n_0 + P)}{T_s N_s (Q - P^2)} \\ \frac{-(n_0 + P)}{T_s N_s (Q - P^2)} & \frac{n_0^2 + 2n_0 P + Q}{N_s (Q - P^2)} \end{bmatrix} \tag{36}$$

where σ^2 is the variance of the uncorrelated real and imaginary components of the i.i.d. zero-mean complex Gaussian noise samples, a is the amplitude of the complex exponential, N_s is the number of samples in the observation, T_s is the sampling period, n_0 is the index of the first sample of the observation in the observer's local time $P := (N_s - 1)/2$, and $Q := (N_s - 1)(2N_s - 1)/6$. This result is used to generate the zero-mean jointly Gaussian constituent estimation errors at each base station with appropriate covariances.

All of the examples in this section (except for Fig. 8) assume that the synchronization beacons and uplink beacon have a duration of 1 ms. After receiving the uplink beacon, the base stations in the participating set $\mathcal{M}_0 = \{1, \ldots, M\}$ then form their downlink carrier phase and frequency estimates and all immediately begin transmitting as a distributed beamformer. The beamforming power at the mobile is computed using (15) and (35) for each realization of the estimation errors and phase noise processes.

Fig. 5 provides a performance comparison among the master-slave, round-trip, and two-way open-loop techniques by plotting the mean received power at the mobile for an $M = 7$ base station network as a function of the elapsed time from the end of the uplink beacon. The mean received power was normalized

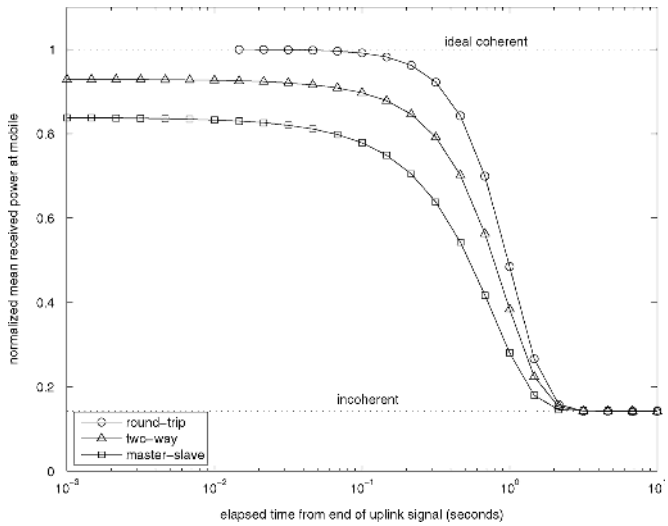

Fig. 5. Normalized mean received power at the mobile as a function of the elapsed time from the end of the uplink signal for the round-trip, two-way, and master-slave retrodirective distributed beamformers with $M = 7$ and $r = 0.01$.

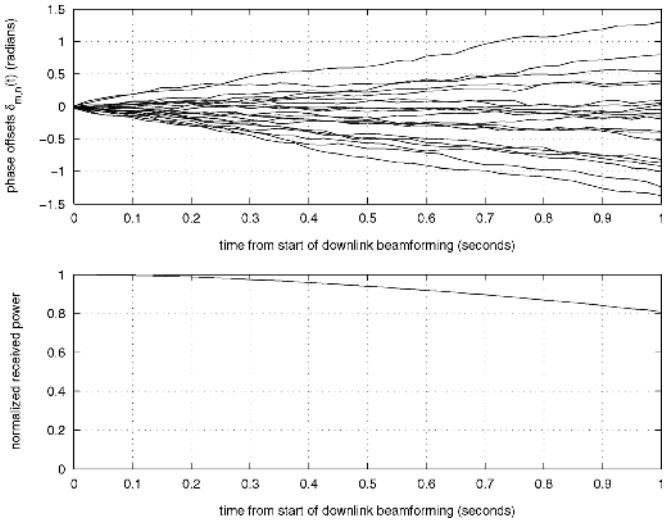

Fig. 6. Pairwise phase offsets $\delta_{m,n}(t)$ and received power as a function of the time from the start of downlink beamforming for one realization of the constituent phase/frequency estimation errors with $M = 7$, all channels with $\mathrm{SNR} = 10$ dB, and $r = 0.01$.

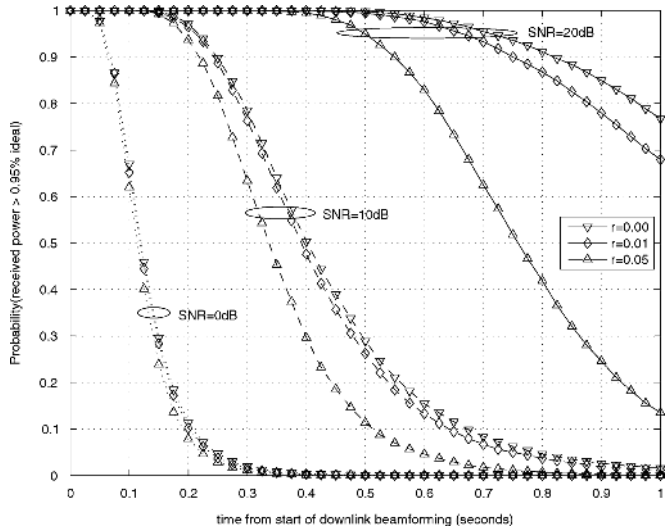

Fig. 7. Probability received power at mobile exceeds 95% of the ideal beamformer received power for an $M = 7$ base station retrodirective distributed downlink beamformer as a function of the time from the start of downlink beamforming for different values of SNR and phase noise parameter r.

by the ideal beamforming power $M^2 = 49$. The signal–to-noise ratio (SNR) $\mathrm{SNR} = 10\log_{10}(a^2/\sigma^2)$ was assumed to be 10 dB for all synchronization beacons exchanged between base stations and 3 dB for the uplink beacon from the mobile. The phase noise parameter was set to $r = 0.01$. Note that the round-trip technique does not begin transmitting until 12 ms after the end of the uplink beacon due to the fact that the round-trip protocol exchanges beacons among the base stations *after* the reception of the uplink beacon, as discussed in Section I. The two-way and master-slave synchronized base stations are synchronized *prior* to the reception of the uplink beacon, hence they can begin beamforming immediately. In this example, two-way and master-slave synchronization was performed 0.5 seconds prior to the transmission of the uplink beacon. This delay combined with the unavoidable frequency offset and oscillator phase noise has caused the two-way and master-slave synchronized base stations to drift slightly out of phase over the time prior to the start of beamforming, resulting in some loss of performance at the start of beamforming with respect to the ideal bound. Nevertheless, the two-way synchronized distributed beamformer offers a normalized mean received power within 0.1 to 0.15 (corresponding to a loss of less than 1 dB) of the round-trip distributed beamformer (and outperforms the master-slave synchronized distributed beamformer by a similar margin) in this example despite having been synchronized 0.5 seconds prior to the transmission of the uplink beacon from the mobile.

Fig. 6 is an $M = 7$ base station example of the pairwise phase offsets $\delta_{m,n}(t)$ in a network of two-way synchronized base stations and the received power at the mobile (normalized by the ideal beamforming power $M^2 = 49$) at the mobile as a function of the elapsed time from the start of beamforming for the case when the uplink beacon is received immediately after the last base station is synchronized. The SNR $\mathrm{SNR} = 10\log_{10}(a^2/\sigma^2)$ was assumed to be identical for all beacon observations at all base stations, including the uplink, and was set to 10 dB. The phase noise parameter was set to $r = 0.01$.

The upper part of Fig. 6 shows the effect of each of the three components of the pairwise phase offset in (17) for a single realization of the estimation errors and phase noise processes. The pairwise phase offset $\tilde{\phi}_{m,n}$ appears as the initial phase difference between the base stations at the start of beamforming. The pairwise frequency offset $\tilde{\omega}_{m,n}$ is visible in the linear phase drift between the base stations. The pairwise phase noise offset $\chi_m(t) - \chi_n(t)$ is evidenced in the random fluctuations of the pairwise offsets around the linear trajectories. As expressed in (15) and shown in the lower part of Fig. 6, the aggregate effect of these pairwise offsets is an inevitable reduction in the received power at the mobile with respect to the ideal prediction. The distributed transmit beamforming power remains above 95% of the ideal for approximately 0.45 seconds in this example.

Fig. 7 is an $M = 7$ base station example showing the probability that the distributed downlink beamforming power at elapsed time t_{bf} from the start of beamforming exceeds 95% of the ideal beamforming power at the mobile for three different SNRs and three different values of the phase noise parameter r for the case when the uplink beacon is transmitted immediately after the last base station is synchronized. The synchronization beacon and uplink beacon durations were all set to 1 ms. These results show that two-way synchronization can enable the base stations to form a high-quality distributed downlink beamformer with high probability when the SNR is high and when r is small. The phase noise parameter r is of less importance when the SNR is low since, in this case, performance degradation is caused primarily by estimation error rather than SLO phase noise. Nevertheless, the results in Fig. 7 show that the time the distributed beamformer exceeds 95% of the ideal beamforming power at the mobile can be on the order of hundreds of milliseconds, with high probability, even in moderate SNR channels with practical oscillators. These results also show that the base stations must be periodically resynchronized in order to maintain an acceptable level of

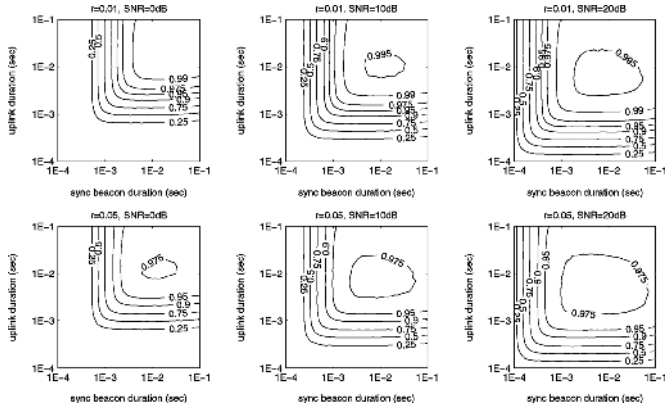

Fig. 8. Normalized mean received power at the mobile as a function of synchronization beacon duration and uplink beacon duration for an $M = 7$ base station retrodirective distributed downlink beamformer when the elapsed time from the start of downlink beamforming $t_{\rm bf} = 0.5$.

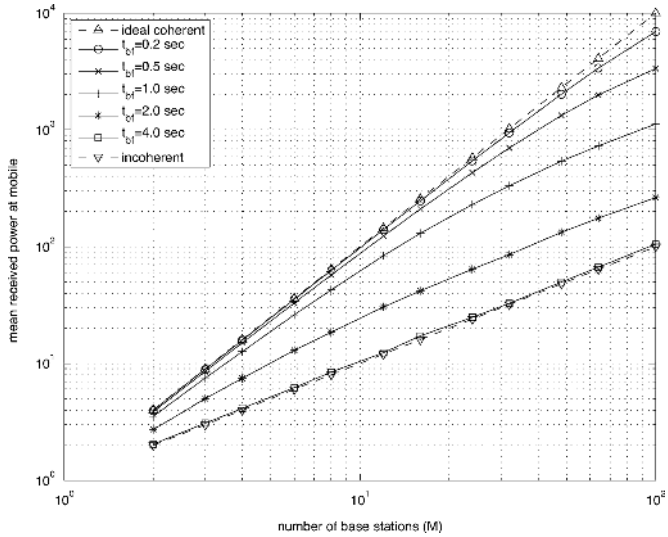

Fig. 9. Mean received power at the mobile as a function of the number of base stations M for different values of time from the start of retrodirective downlink beamforming ($t_{\rm bf}$) for 10 dB SNR beacons and $r = 0.01$. The "ideal coherent" upper bound corresponds to perfect transmit phase and frequency synchronization with no phase noise. The "incoherent" lower bound corresponds to random transmit phases.

performance with high probability. In this example, resynchronization requires 12 ms, implying that the synchronization overhead is small with respect to the expected useful duration of the distributed beamformer.

Fig. 8 shows the effect of the synchronization beacon durations and uplink beacon duration on the mean received power of the distributed downlink beamformer at the mobile for three different SNRs and two different phase noise parameters r for the case when the uplink beacon is transmitted immediately after the last base station is synchronized. The mean received power at the mobile in this example was computed at $t_{\rm bf} = 0.5$ seconds from the start of beamforming. These results show that if either beacon duration is too short, the mean received beamforming power at the mobile will be a small fraction of the ideal beamforming power. Intuitively, this is because a short beacon results in relatively large estimation errors and any large estimation error (either during synchronization or in the uplink beacon) significantly diminishes the ability of the distributed beamformer to remain synchronized until $t_{\rm bf} = 0.5$. These results suggest that, when the SNR of each channel is identical, the best performance is achieved when the synchronization beacon duration is approximately the same as the uplink beacon duration. Fig. 8 also shows that the mean received beamforming power does not monotonically increase with either beacon duration. For example, in the case when $r = 0.05$ and $\mathrm{SNR} = 0$ dB, the maximum mean received beamforming power is obtained when the synchronization beacon durations and the uplink beacon duration are approximately 10^{-2} seconds. If longer beacon durations (either synchronization or uplink) are used, the mean received beamforming power at the mobile decreases somewhat because of the carrier drift and increased phase offset at the start of beamforming.

Fig. 9 shows the effect of the number of participating base stations on the mean received power of the distributed downlink beamformer at the mobile. Intuitively, increasing the number of participating base stations increases the potential beamforming power gain since the ideal beamforming power gain scales according to M^2. As M increases, however, the amount of time spent synchronizing the base stations also increases. This causes increased accumulation of phase and frequency estimation errors and, consequently, increased phase offset at the start of beamforming and increased frequency offset during beamforming. Fig. 9 plots the mean received power at the mobile versus M for several elapsed times $t_{\rm bf}$ after the start of beamforming for the case when all beacons are observed at 10 dB SNR, $r = 0.01$, and the uplink beacon is transmitted immediately after the last base station is synchronized.

The results in Fig. 9 show that increasing the number of base stations participating in the distributed downlink beamformer always increases the mean received power at the mobile, but with diminishing returns. As a specific example, when the elapsed time from the start of beamforming is one second, the mean received power of the distributed downlink beamformer is close to that of the ideal beamformer for $M < 10$. The slope of the mean received power in this region is close to two, indicating that the passband signals are coherently combining at the mobile. In the region where $M \geq 50$, however, the slope of the mean received power curve goes from two to one, indicating that the passband signals are incoherently combining at the mobile. As the beamforming time becomes large, e.g., 5 seconds, the passband signals incoherently combine at the mobile for any value of M. This again demonstrates the need for periodic resynchronization in distributed beamforming systems.

VI. Conclusion

This paper presented a new two-way carrier synchronization protocol to facilitate coordinated multicell retrodirective downlink beamforming. The two-way base station synchronization protocol was developed for a system model in which each base station's local time differs from that of the other base stations in the network. All processing is performed using only local observations in local time at each base station. An analysis of the

statistical properties of the phase and frequency estimation errors and resulting power of a distributed downlink beamformer was also provided. Numerical examples characterizing the performance of multicell retrodirective downlink beamforming in a system using two-way synchronization were presented and demonstrated that near-ideal beamforming performance can be achieved with low synchronization overhead.

REFERENCES

[1] D. Wong and T. J. Lim, "Soft handoffs in CDMA mobile systems," *IEEE Pers. Commun.*, vol. 4, no. 6, pp. 6–17, Dec. 1997.

[2] C. Chow, B. Shraiman, A. Sengupta, and M. Andrews, "Using phase and amplitude control across networks to increase capacity up to fourfold," in *Proc. URSI Nat. Radio Sci. Meet.*, Boulder, CO, Jan. 9–11, 2002, pp. C1–C5.

[3] H. Skjevling, D. Gesbert, and A. Hjorungnes, "A low complexity distributed multibase transmission scheme for improving the sum capacity of wireless networks," in *Proc. IEEE Signal Process. Adv. Wireless Commun. (SPAWC)*, Jun. 2007, pp. 1–5.

[4] H. Dahrouj and W. Yu, "Coordinated beamforming for the multicell multiantenna wireless system," in *Proc. Conf. Inf. Sci. Syst. (CISS)*, Mar. 2008, pp. 429–434.

[5] S. Shamai and B. M. Zaidel, "Enhancing the cellular downlink capacity via co-processing at the transmitting end," in *Proc. IEEE Veh. Technol. Conf. (VTC)*, 2001, vol. 3, pp. 1745–1749.

[6] H. Zhang and H. Dai, "Cochannel interference mitigation and cooperative processing in downlink multicell multiuser mimo networks," *EURASIP J. Wireless Commun. Netw.*, vol. 2004, no. 2, pp. 222–235, Dec. 2004.

[7] M. Karakayali, G. Foschini, R. Valenzuela, and R. Yates, "On the maximum common rate achievable in a coordinated network," in *Proc. IEEE Int. Conf. Commun.*, Jun. 2006, vol. 9, pp. 4333–4338.

[8] M. Karakayali, G. Foschini, and R. Valenzuela, "Network coordination for spectrally efficient communications in cellular systems," *IEEE Wireless Commun.*, vol. 13, no. 4, pp. 56–61, Aug. 2006.

[9] G. Foschini, K. Karakayali, and R. Valenzuela, "Coordinating multiple antenna cellular networks to achieve enormous spectral efficiency," *IEE Proc. Commun.*, vol. 153, no. 4, pp. 548–555, Aug. 2006.

[10] S. Jing, D. N. C. Tse, J. B. Soriaga, J. Hou, J. E. Smee, and R. Padovani, "Multicell downlink capacity with coordinated processing," *EURASIP J. Wireless Commun. Netw.*, vol. 2008, 2008.

[11] V. Jungnickel, L. Thiele, T. Wirth, T. Haustein, S. Schiffermuller, A. Forck, S. Wahls, S. Jaeckel, S. Schubert, H. Gabler, C. Juchems, F. Luhn, R. Zavrtak, H. Droste, G. Kadel, W. Kreher, J. Mueller, W. Stoermer, and G. Wannemacher, "Coordinated multipoint trials in the downlink," in *Proc. IEEE GLOBECOM Workshops*, Dec. 2009, pp. 1–7.

[12] V. Jungnickel, T. Wirth, M. Schellmann, T. Haustein, and W. Zirwas, "Synchronization of cooperative base stations," in *Proc. IEEE Int. Symp. Wireless Commun. Syst. (ISWCS)*, Oct. 2008, pp. 329–334.

[13] C. Pon, "Retrodirective array using the heterodyne technique," *IEEE Trans. Antennas Propag.*, vol. 12, no. 2, pp. 176–180, Mar. 1964.

[14] R. D. Preuss and T. P. Bidigare, "Methods and Systems for Distributed Synchronization," U.S. Patent Appl. 12/383,192, Mar. 19, 2009.

[15] D. R. Brown III and H. V. Poor, "Time-slotted round-trip carrier synchronization for distributed beamforming," *IEEE Trans. Signal Process.*, vol. 56, no. 11, pp. 5630–5643, Nov. 2008.

[16] R. Mudumbai, G. Barriac, and U. Madhow, "On the feasibility of distributed beamforming in wireless networks," *IEEE Trans. Wireless Commun.*, vol. 6, no. 5, pp. 1754–1763, May 2007.

[17] N. J. Boucher, *The Cellular Radio Handbook*, 4th ed. New York: Wiley-Intersci., 2001.

[18] A. Rosenberg and S. Kemp, *CDMA Capacity and Quality Optimization*. New York: McGraw-Hill, 2003.

[19] G. Fettweis, E. Zimmermann, V. Jungnickel, and E. Jorswieck, "Challenges in future short range wireless systems," *IEEE Veh. Technol. Mag.*, vol. 1, no. 2, pp. 24–31, 2006.

[20] D. Parish, F. Farzaneh, and C. Barrat, "Methods and Apparatus for Calibrating Radio Frequency Base Stations Using Antenna Arrays," U.S. Patent 6 037 898, Oct. 1997.

[21] A. Bourdoux, B. Come, and N. Khaled, "Non-reciprocal transceivers in OFDM/SDMA systems: Impact and mitigation," in *Proc. Radio and Wireless Conf. RAWCON'03*, 10–13, 2003, pp. 183–186.

[22] M. Guillaud, D. Slock, and R. Knopp, "A practical method for wireless channel reciprocity exploitation through relative calibration," in *Proc. 8th Int. Symp. Signal Process. Appl.*, Aug. 2005, vol. 1, pp. 403–406.

[23] E. Baghdady, R. Lincoln, and B. Nelin, "Short-term frequency stability: Characterization, theory, and measurement," *Proc. IEEE*, vol. 53, no. 7, pp. 704–722, Jul. 1965.

[24] D. Rife and R. Boorstyn, "Single-tone parameter estimation from discrete-time observations," *IEEE Trans. Inf. Theory*, vol. 20, no. 5, pp. 591–598, Sep. 1974.

[25] D. Gerlach and A. Paulraj, "Adaptive transmitting antenna arrays with feedback," *IEEE Signal Process. Lett.*, vol. 1, no. 10, pp. 150–152, Oct. 1994.

[26] P. Zetterberg and B. Ottersten, "The spectrum efficiency of a base station antenna array system for spatially selective transmission," *IEEE Trans. Veh. Technol.*, vol. 44, no. 3, pp. 651–660, Aug. 1995.

[27] J. C. Eidson, *Measurement, Control, and Communication Using IEEE 1588*. New York: Springer, 2006.

[28] K. Leong, Y. Wang, and T. Itoh, "A full duplex capable retrodirective array system for high-speed beam tracking and pointing applications," *IEEE Trans. Microw. Theory Tech.*, vol. 52, no. 5, pp. 1479–1489, May 2004.

[29] A. Demir, A. Mehrotra, and J. Roychowdhury, "Phase noise in oscillators: A unifying theory and numerical methods and characterization," *IEEE Trans. Circuits Syst. I: Fund. Theory Appl.*, vol. 47, no. 5, pp. 655–674, May 2000.

[30] J. A. McNeill and D. Rickets, *The Designer's Guide to Jitter in Ring Oscillators*. New York: Springer, 2009.

[31] H. V. Poor, *An Introduction to Signal Detection and Estimation*, 2nd ed. New York: Springer-Verlag, 1994.

Robert D. Preuss (S'82–M'83–SM'99) received the A.B. degree in mathematics and the M.S. degree in applied mechanics from Baston University, Boston, MA, in 1975 and 1977, respectively.

He is currently a Lead Scientist at Raytheon BBN Technologies, Cambridge, MA. Before joining BBN in 1986, he received a 1982 NASA Certificate of Recognition and, during the 1984–1985 academic year, he served as a Fulbright professor in Tampere Finland. He has made contributions in diverse technical areas including: boundary element methods for computational aerodynamics, modified DSSS communication methods for audio steganography, fast algorithms to solve large ill-conditioned linear systems (arising in the design of MIMO vibration control systems) by exploiting the SPD tensor-convolution block-Toeplitz matrix structure, and advanced speech spectral envelope estimation methods for noise-robust low-data-rate voice coding systems. His current interests also include the study of human molecular genetics for targeted treatment of cancer.

D. Richard Brown, III (S'97–M'00–SM'09) received the B.S. and M.S. degrees from The University of Connecticut, Storrs, in 1992 and 1996, respectively, and the Ph.D. degree from Cornell University, Ithaca, NY, in 2000, all in electrical engineering.

He was a Development Engineer at the General Electric Company, Plainville, CT, from 1992 to 1997. He is currently an Associate Professor at Worcester Polytechnic Institute, Worcester, MA. His current research interests include synchronization and distributed communication techniques.